

Robot-Assisted FBG-based Sensorized Needle Calibration

Final Report

EN. 601.656 Advanced Computer Integrated Surgery

Kefan Song

M.S.E student, Biomedical Engineering Department

ksong13@jhu.edu

Mentors: Dr. Iulian Iordachita, Dimitri Lezcano, Ge Sun

Table of Contents

1. Clinical Motivation.....	2
2. Prior Work.....	2
3. Objectives	2
4. Current Manual Procedures.....	2
5. Technical Approach	3
a. Calibration Platform.....	4
b. Algorithm.....	5
6. Results.....	6
7. Discussion and Future Directions	8
8. Deliverables.....	8
9. Dependencies.....	9
10. Timeline	9
11. Team Members	10
12. Management Plan	10
13. Reading List.....	10
14. References	11

1. Clinical Motivation

The motivation of the project comes from current procedures in prostate biopsy and brachytherapy, of which a stiff needle is inserted manually to the targeted region in the prostate tissue with guidance of an ultrasound probe either to retrieve a slice of potential cancerous tissue or to implant radioactive seeds into the tissue. This approach is problematic as ultrasound is inadequate for visualization of cancerous region or the seeds to be implanted. In addition, it is common that the prostate rotates and deforms during the insertion of the needle, which often causes displacement of the target region. In this situation, the straight needle trajectory becomes insufficient, and will often result in poor accuracy and poor repeatability of the insertion. Thus, an updated approach was proposed, which includes inserting a flexible needle using robotic assistance with real-time MRI image guidance.

2. Prior Work

The flexible bevel tip needle was chosen to be the needle for the updated approach mentioned in the previous section, and FBG sensors are attached to the inside of the needle to constantly monitor its curvature. Since then, a lot of progress has been made in generating various mathematical models and algorithms for the needle, including real-time needle navigation algorithm, shape determination model, and trajectory generation algorithm. In addition, a manual calibration procedure has been setup for the needles to precisely and consistently calculate the curvature value of the needle from the FBG sensor readings. However, as the needles are very sensitive, the current calibration procedure is very time consuming and can take several hours for each needle, and even with the careful handling of the needle the calibration process is still prone to human error.

3. Objectives

As mentioned in the previous section, the current manual calibration process of the FBG based sensorized needle is time consuming and subject to human error. Thus, the goal of this project is to build a robotic system for (semi)automatic calibration of flexible needles with FBG-based shape-sensing capabilities. It is hypothesized that the robot-assisted needle calibration would optimize needle construction and improve its shape-sensing accuracy.

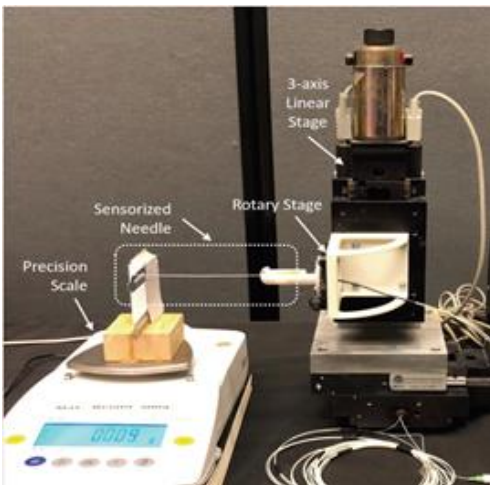
4. Current Manual Procedures

According to the current manual calibration procedure, two sets of tests need to be performed to calibrate every FBG needle: the characterization of the needle and the calibration of the needle. The characterization of the needle aims to validate that the wavelength shift of the FBG sensors inside the needle is proportional to the bending distance of the needle, as this is the fundamental mechanism in using the FBG reading to determine the needle's bending angle. The bending distance is defined as the tangential distance between the tip and the base of the needle. If a needle does not pass the characterization test, meaning that its readings do not satisfy a linear relationship with its bending distance, then this needle can be determined to have faulty measurements, and no further testing would be necessary. If a needle passes the characterization test, however, it will then go through a calibration process to obtain its calibration matrices. The set of calibration matrices obtained will then be verified before it is recorded as the property of that specific needle. The current manual procedure setup is as follows.

To perform the characterization of the needle manually, the needle tip is first fixed on a horizontal bar that is attached to a precision scale (Figure 01 A). The needle location is then adjusted vertically so that the scale reading is zero while the needle tip is still touching the horizontal bar. This is to make sure that the bending distance of the needle is zero at the beginning of the test. Then the needle is pressed down on the scale in 10 repetitions of 1 mm increments. After each increment 200 datapoints are collected from the needle. Then the needle is released upwards for 10 repetitions of 1mm increments as well, with the same amount of datapoints collected after each increment. This is defined as one load-unload cycle, and such cycle is to be repeated for 5 times to conclude the data collection process. To fully validate the needle, such characterization process needs to be performed for each and every FBG channel of the needle, with the channel to be tested located at the bottom of the needle. To visualize the characterization results, the FBG wavelength shift is plotted against the needle bending distance, and compared to linear fitted lines.

For the calibration process, the needle is inserted repetitively into slots with predetermined constant curvatures on a calibration jig (Figure 01 B). The insertion process is repeated 10 times for each single slot, and with the needle rotated at 0, ± 90 , and 180 degrees along its axial direction. The calibration matrix for each active area of the needle can then be calculated through least-squares fit between the FBG data and the curvature data.

A



B

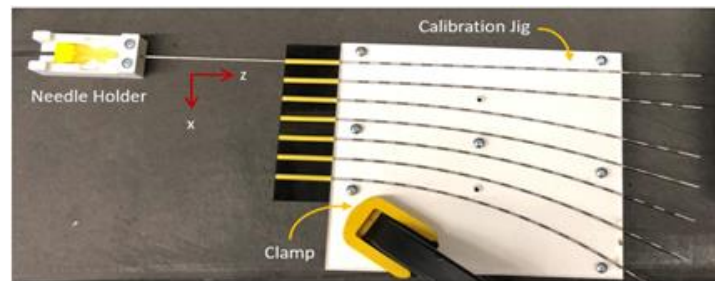


Figure 01. A. Manual characterization and B. calibration processes of FBG needles.

5. Technical Approach

The robotic system was built to perform both characterization and calibration processes automatically. The setup of the system is shown in Figure 02. The entire building process was divided into two portions, the hardware portion, which is the calibration platform, and the software portion, which is the algorithm to control the movement of the robotic system as well as collecting data.

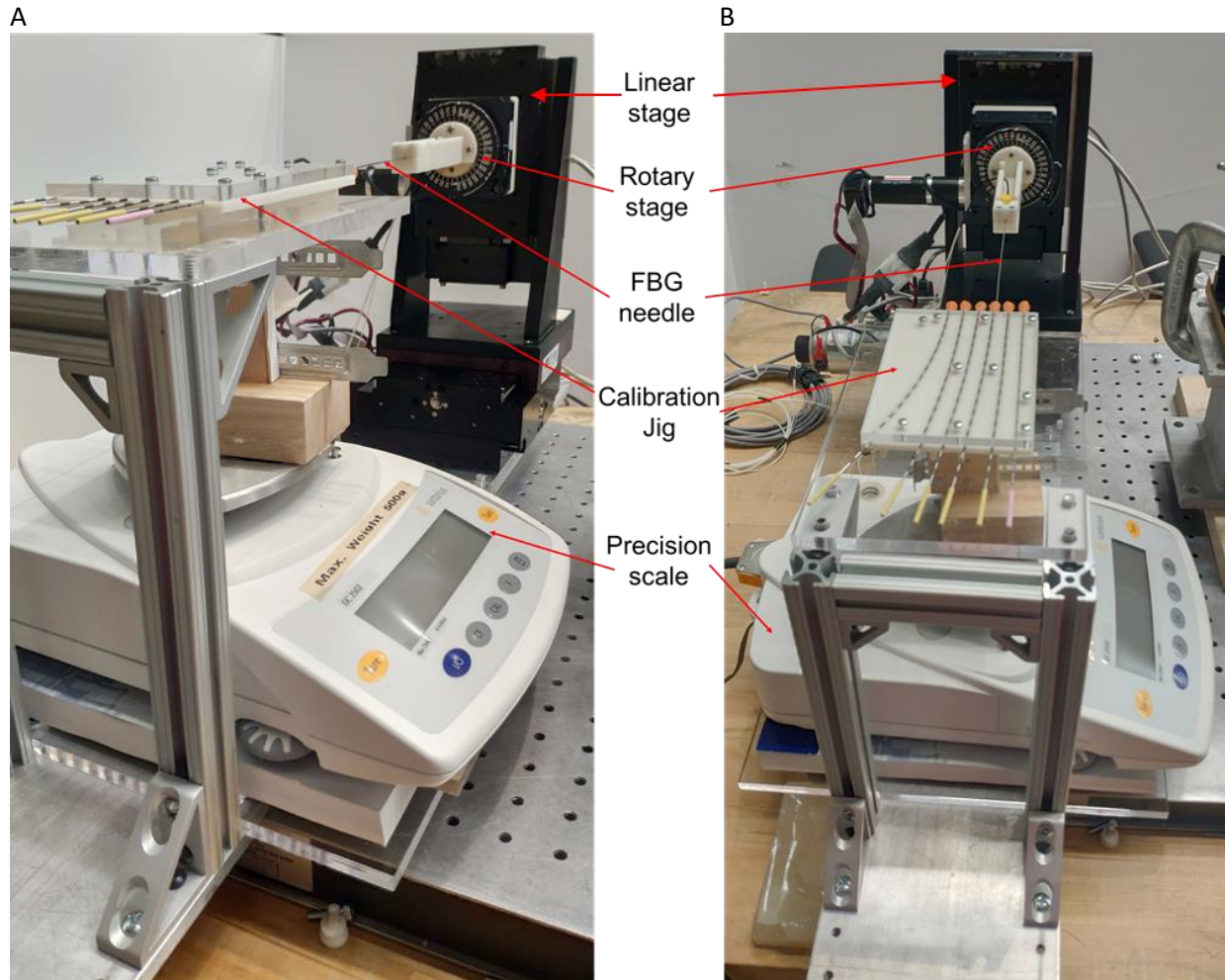


Figure 02. A. Side view and B. top view of the robotic calibration system.

a. Calibration Platform

According to the current calibration procedure, two types of testing are needed to fully calibrate a needle, so a calibration platform was built to have the correct setup for both testing processes. Based on that, the calibration platform is divided into three sections: the robotic needle holder, the characterization station, and the calibration station.

The robotic needle holder section consists of a 3D linear stage, a rotary stage, and a 3D printed needle holder, and its goal is to move the needle to the corresponding stations and perform the tests. At the characterization station, there's a precision scale with a custom-made piece glued to its weighing platform. The purpose of the piece is to provide a heightened platform of which the needle tip can be fixed at. The calibration station, which is directly on top of the characterization station, consists of a calibration jig with multiple slots of predetermined constant curvature. The entire platform is supported by aluminum profiles and acrylic plates, as well as a base platform.

b. Algorithm

The overall workflow of the algorithm is shown in Figure 04, in which the operations in red are automatic robot movements, the operations in grey are data collections, and the operation in green, which is the initial calibration of the platform, is the only operation that needs to be performed entirely manually. In addition, there are two operations with red asterisks, indicating that these operations need occasional manual interference.

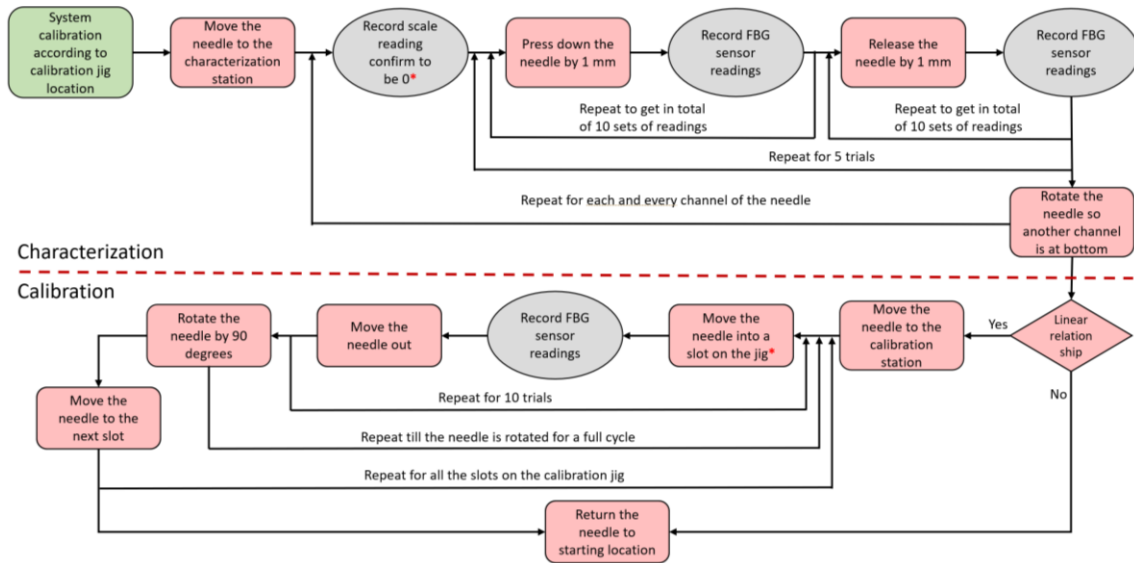


Figure 03. Workflow of the algorithm for the robotic arm movement.

The two operations that need occasional manual interference are both due to limitations of the hardware that's available. The first operation is to confirm that the scale reading is zero. The manual portion of the operation is in calibrating the precision scale. As the scale was meant to be used for static measurements, it will experience some drift in measurements as the characterization process is conducted. On the other hand, as the FBG needles are likely not perfectly straight, it is possible that the location with zero bending distance will shift as well. Thus, it is necessary to use the precision scale readings to reconfirm the zero-reading point every time after the needle is rotated, and it is also necessary to tare the scale every time beforehand. Currently this step is still performed manually, and is considered acceptable as it only involves pushing the "tare" button on the scale.

The other operation that needs manual interference is when inserting the needle into the slots on the calibration jig. This step is actually always the most tricky part of the calibration process, because the slots are pretty closely fitted to the needle, and a slight mismatch during insertion of the needle tip will result in a complete failure. Currently at the entry points of the calibration slots there are funnel shaped guides (orange pieces in Figure 02 right) in hopes of helping to guide the needle during insertion process, but the effect of the guides are not ideal. Thus, for the current prototype, manual guidance is still needed for the needle to be successfully inserted into each calibration slots. Luckily it is not as heavy of a workload as it is in the manual calibration process, because the needle tip will actually remain in the calibration slot during the repetitive insertion and

retraction steps. Therefore during the entire calibration process there are only six instances where the needle needs manual guidance, which are the initial insertions to each calibration slot.

6. Results

After the system was built and debugged, one set of needle calibration process was conducted on an FBG-sensorized needle, and the results are reported.

First of all, the entire needle calibration process took in total 2 hours and 35 minutes, with the characterization process taking 20 minutes and the calibration process taking 2 hours and 15 minutes. This total time span is comparable to the manual process, which usually takes 30 minutes for needle characterization, and about 2 hours for needle calibration. However, the time that needed human interaction was greatly reduced. For manual calibration process, almost the entire 2 hours and 30 minutes require manual operation, whereas during the robotic process, manual operation is only required for three times of scale taring and six times of needle insertion guidance, which takes about 30 seconds each and 1 minute each, respectively. Thus, even though the robotic calibration system is not entirely automatic, it doesn't require any human attention for the vast majority of the testing process, thus saving a lot of time for operators of the calibration process.

As for the results from the entire calibration procedure, the robotic system is able to output similar results to the results obtained from manual calibration. For the characterization process, it is able to output the wavelength shift for each active area of every channel in every single trial (Figure 04.A), the average wavelength shift of all active areas across the same channel (Figure 04.B), and the average wavelength shift of all channels at a specific active area (Figure 04.C) with respect to the bending distance. For the calibration process, it is able to plot the relationship between the wavelength shift of each channel at a single active area and the planar curvature of the needle (Figure 04.D).

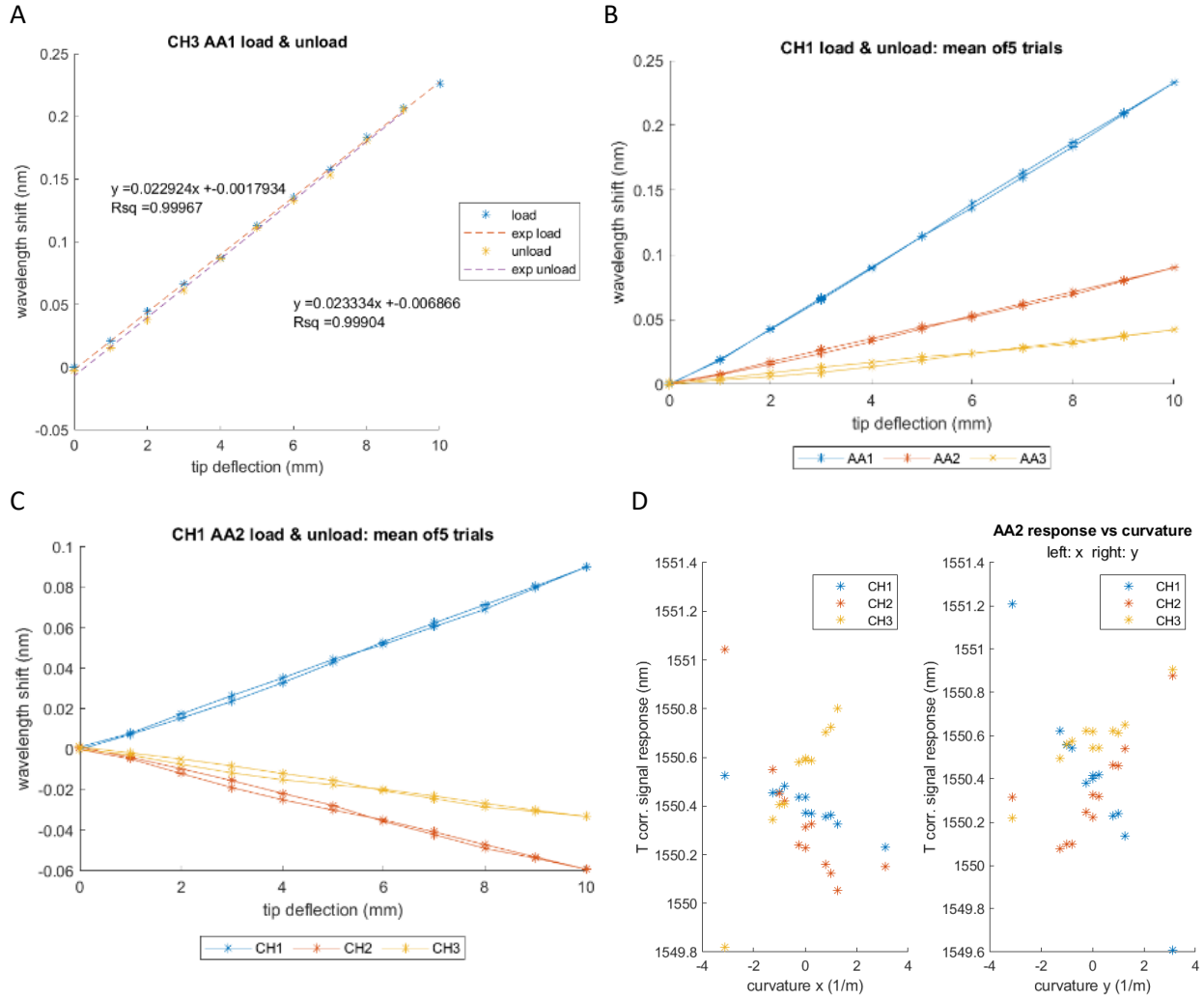


Figure 04. A. Sample plot of wavelength shift of a specific channel at an active area with respect to the bending distance; B. Sample plot of wavelength shift of a specific channel at all active areas with respect to the bending distance; C. Sample plot of wavelength shift of all channels at a specific active area with respect to the bending distance; D. Sample plot of wavelength shift of all channels at a specific active area with respect to the planar curvature of the needle.

Apart from the plots, the system is also able to output the calibration matrices for each active area of the needle, as shown in Figure 05. This set of calibration matrices can then be treated as the property of this specific needle after it is validated.

$$C1_{rob} = \begin{bmatrix} -1.5283 & -3.7178 \\ -2.5518 & 3.6508 \\ 4.0791 & 0.0670 \end{bmatrix}$$

$$C2_{rob} = \begin{bmatrix} -0.3211 & -2.7145 \\ -2.1057 & 1.8308 \\ 2.4265 & 0.8837 \end{bmatrix}$$

$$C3_{rob} = \begin{bmatrix} -0.8032 & -4.0764 \\ -3.6630 & 2.2644 \\ 4.4657 & 1.8127 \end{bmatrix}$$

Figure 05. Resulting calibration matrices for the sample needle obtained from the calibration system.

7. Discussion and Future Directions

Even though the calibration system is able to output a set of results for a given needle, it still lacks the validation process to justify the results. On the other hand, it is clear from Figure 04 that there are errors presented in the plots. Thus, it is necessary to perform validation of the needle in the future to justify the results, and the validation process can be performed by inserting the needle into a set of slots with different curvatures, using the calibration matrices to predict the curvatures of the slot, and checking whether the predicted curvature values match the actual curvatures of the slots.

Another major direction for the development of this system is to explore possible sources of errors through repetitive calibration experiments. Currently some suspected error sources include loosened component, slightly tilted calibration jig platform and inaccurate calibration jig curvature, and these all must be verified and reduced in the future.

Last but not least, it is also important to improve the system so the entire system can be fully automatic, and it could be done by researching deeper into communication between Matlab and the precision scale, as well as better design for funnel-shaped needle guidance for the calibration slots.

8. Deliverables

The updated deliverables of the project are listed in Figure 06. It is divided into the minimum, expected and maximum deliverables. Essentially, the minimum deliverable is able to perform a needle calibration with reduced human error but still require extensive user interaction. The expected deliverable is to perform automatic calibration and the maximum deliverable is to compare the accuracy and sources of errors between the robotic calibration and manual calibration, as well as generating a conference paper base on the project.

In the end, only most of the expected deliverables were finished. The example calibration video was planned under the initial impression that the robotic system can significantly reduce the time needed for needle calibration, and was eventually canceled as the calibration process still takes more than 2 hours. A quick comparison between robotic and manual calibration processes were conducted by comparing the calibration matrices obtained from the two processes, but more structural and more in

depth comparison is still lacked. The conference paper will be finished after the end of the semester due to the extension of the paper submission deadline.

	Hardware	Algorithm	Experiment data	Documentation
Minimum	Calibration platform	Semi-automatic code (manual movement between jigs + manual needle rotation) with comments	Calibration matrices for one needle	User manual for the system
Expected		Automatic code with comments		Updated user manual and example calibration video
Maximum			Comparison of robotic calibration and manual calibration	A conference paper based on this project

Figure 06. Deliverables of the project.

9. Dependencies

The updated dependencies of the project are listed in Figure 07. All dependencies have been acquired except for one, for which the contingency plan was executed and the progress of the project was not affected at all.

Dependency	Status	Contingency plan	Planned DDL	Hard DDL
Acquire robotic arm and data acquisition unit	Acquired	Both robot and the data acquisition unit have a backup model	Feb 19	Feb 19
Several needles for testing	Acquired	Currently the lab has multiple needles	Feb 19	Feb 19
Curvature jig model	Acquired	More models can be 3D printed fairly quickly	Feb 19	Feb 19
Lab access	Acquired	N/A	Feb 12	Feb 12
Aluminum breadboard	Acquired	Multiple backup choices including acrylic base and aluminum profiles	Feb 25	March 12
Substitute force sensing mechanism for precision scale	Not acquired	Continue using the scale	March 29	N/A
Aluminum profiles & accessories	Acquired	Buy from other vendors	March 26	Apr 6
Acrylic sheet	Acquired	Use scraps from lab	March 26	Apr 6
DB-9 cables	Acquired	Use existing cables from another robot	March 26	Apr 6

} Newly added

Figure 07. Dependencies of the project.

10. Timeline

The actual timeline of the project is shown in Figure 08 with the actual completion date for the deliverables. Unfortunately the maximum deliverables couldn't be completed before the end of the semester, but the project will be carried on throughout the summer.

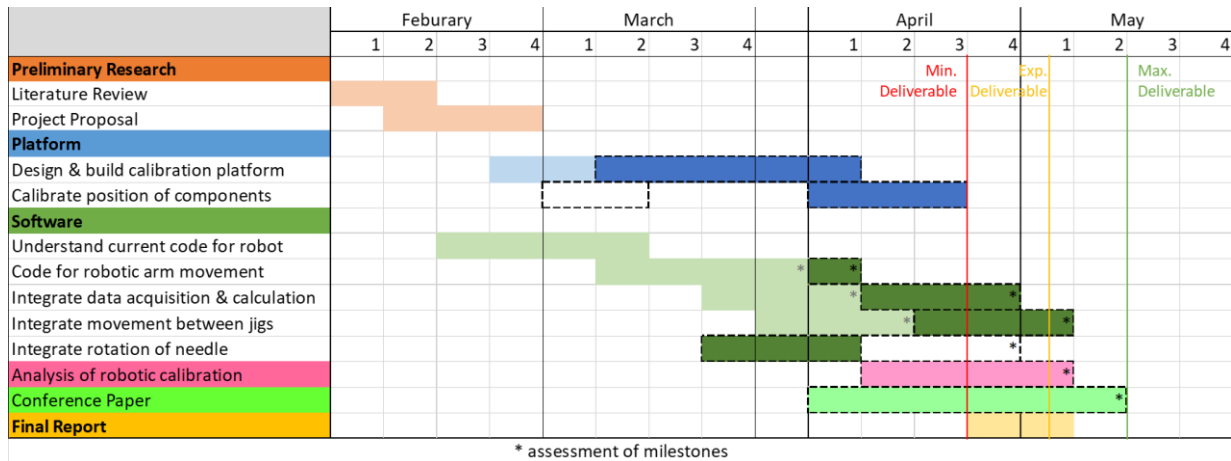


Figure 08. Timeline of the project.

11. Team Members

Kefan Song is the only member of the team and is responsible for all tasks required for this project. The mentors of the team include:

Dr. Iulian Iordachita: principal investigator of the project.

Dimitri Lezcano: primary mentor of the project.

Ge Sun: Mentor on robot control and needle calibration steps.

12. Management Plan

The management plan include weekly meetings and in-person interactions. The team will meet weekly on Fridays via Zoom in which the team member will report the weekly progress of the project. In addition, there will be ad hoc in-person interaction in the lab for specific problems that come up.

All 3D models of the calibration platform are stored in JHU OneDrive and can be accessed through this link: https://livejohnshopkins-my.sharepoint.com/:f/g/personal/ksong13_jh_edu/EsxNbA9EXphAou5vg-aSnnlBvmqFr06G59T5XKh1rSP8ww?e=KMyiYA

All algorithms for the robotic calibration system are stored in the desktop computer in the LCSR lab and also in JHU OneDrive, and can be accessed through this link: https://livejohnshopkins-my.sharepoint.com/:f/g/personal/ksong13_jh_edu/Er6lbZlzXoNPkyYcbG_IfhMB8ScX01aNe5UM5yTwLxLV3A?e=kFpvfu

13. Reading List

Zhang, L., Li, C., Zhang, X., Liu, G., Liu, Y., Zhao, J., ... & Fan, Y. (2019, December). A New Method For Fiber Bragg Grating Based Needle Shape Sensing Calibration. In 2019 IEEE International Conference on Robotics and Biomimetics (ROBIO) (pp. 1953-1958). IEEE.

Seifabadi, R., Iordachita, I., & Fichtinger, G. (2012, June). Design of a teleoperated needle steering system for MRI-guided prostate interventions. In 2012 4th IEEE Ras & EmbsInternational Conference on Biomedical Robotics And Biomechatronics(Biorob) (pp. 793-798). IEEE.

Sankaran, N. K., Chembrammal, P., & Kesavadas, T. (2020). Force calibration for an endovascular robotic system with proximal force measurement. *The International Journal of Medical Robotics and Computer Assisted Surgery*, 16(2), e2045.

Seifabadi, R., Gomez, E. E., Aalamifar, F., Fichtinger, G., & Iordachita, I. (2013, November). Real-time tracking of a bevel-tip needle with varying insertion depth: Toward teleoperated MRI-guided needle steering. In 2013 IEEE/RSJ International Conference on Intelligent Robots and Systems (pp. 469-476). IEEE.

Kim, J. S., Guo, J., Chatrasingh, M., Kim, S., & Iordachita, I. (2017, September). Shape determination during needle insertion with curvature measurements. In 2017 IEEE/RSJ International Conference on Intelligent Robots and Systems (IROS) (pp. 201-208). IEEE.

Lezcano, D. A., Iordachita, I. I., & Kim, J. S. (2020, October). Trajectory Generation of FBG-SensorizedNeedles for Insertions into Multi-Layer Tissue. In 2020 IEEE Sensors (pp. 1-4). IEEE.

Kim, J. S., Chatrasingh, M., Kim, S., Suthakorn, J., & Iordachita, I. I. (2017, December). Fiber Bragg Grating based needle shape sensing for needle steering system: Evaluation in inhomogeneous tissue. In 2017 IEEE SENSORS (pp. 1-3). IEEE.

Henken, K. R., Dankelman, J., van den Dobbelsteen, J. J., Cheng, L. K., & van der Heiden, M. S. (2013). Error analysis of FBG-based shape sensors for medical needle tracking. *IEEE/ASME Transactions on mechatronics*, 19(5), 1523-1531.

Galloway, K. C., Chen, Y., Templeton, E., Rife, B., Godage, I. S., & Barth, E. J. (2019). Fiber optic shape sensing for soft robotics. *Soft robotics*, 6(5), 671-684.

Chen, X., Yi, X., Qian, J., Zhang, Y., Shen, L., & Wei, Y. (2020). Updated shape sensing algorithm for space curves with FBG sensors. *Optics and Lasers in Engineering*, 129, 106057.

14. References

Seifabadi, R., Gomez, E. E., Aalamifar, F., Fichtinger, G., & Iordachita, I. (2013, November). Real-time tracking of a bevel-tip needle with varying insertion depth: Toward teleoperated MRI-guided needle steering. In 2013 IEEE/RSJ International Conference on Intelligent Robots and Systems (pp. 469-476). IEEE.

Kim, J. S., Guo, J., Chatrasingh, M., Kim, S., & Iordachita, I. (2017, September). Shape determination during needle insertion with curvature measurements. In 2017 IEEE/RSJ International Conference on Intelligent Robots and Systems (IROS) (pp. 201-208). IEEE.

Lezcano, D. A., Iordachita, I. I., & Kim, J. S. (2020, October). Trajectory Generation of FBG-SensorizedNeedles for Insertions into Multi-Layer Tissue. In 2020 IEEE Sensors (pp. 1-4). IEEE.

Kim, J. S., Chatrasingh, M., Kim, S., Suthakorn, J., & Iordachita, I. I. (2017, December). Fiber Bragg Grating based needle shape sensing for needle steering system: Evaluation in inhomogeneous tissue. In 2017 IEEE SENSORS (pp. 1-3). IEEE.

